

# Sensitivity Optimization of Au/Ti Based-SPR Sensor by Controlling Light Incident Wavelength for Gas Sensing Application

Nadhratul Huda Ahmad Khilmy, Wan Maisarah Mukhtar\*, Affa Rozana Abdul Rashid

Faculty of Science and Technology, Universiti Sains Islam Malaysia (USIM), 71800 Bandar Baru Nilai, Negeri Sembilan, Malaysia.

## Article history

Received

1 August 2022

Revised

28 November 2022

Accepted

29 November 2022

Published online

30 November 2022

\*Corresponding author  
wmaisarah@usim.edu.my

## Abstract

Exposure to harmful gases may cause health problems like bone marrow deficiency, which eventually drops the number of red blood cells, causing anemia and many other dangerous diseases. This work was carried out to study the potential development of a highly sensitive Kretschmann-based surface plasmon resonance (SPR) sensor for gas sensing applications using hybrid thin films of gold/titanium (Au/Ti). To optimize the excitation of surface plasmon polaritons (SPP), the light incident wavelength was varied from visible to infrared spectra. The thickness of Au thin film with a refractive index of  $n = 0.1758 + 3.4101k$  was fixed at 50 nm. Meanwhile, the thicknesses of Ti were controlled between 1 nm to 5 nm to optimize the SPR signal. Four different types of gas samples, such as benzene, methane, carbon monoxide, and carbon dioxide, were exposed to the sensor's surface. The proposed Au/Ti-based SPR sensor with thicknesses of Ti within 1 nm to 5 nm using visible and IR wavelengths able to detect various types of gaseous. Apparently, the deployment of infrared wavelength ( $\lambda = 1550$  nm) at Ti thickness of 3 nm resulted in the highest sensitivity up to  $2412.06^\circ/\text{RIU}$  and showed excellent selectivity to differentiate different types of gases. In conclusion, Au/Ti thin films are promising hybrid materials for gas sensing applications. Obviously, the sensor's sensitivity with total hybrid thin films of 53 nm was successfully enhanced as additional material, Ti, coated on the Au thin film's surface.

**Keywords** SPR, Au/Ti, incident wavelength, Kretschmann, gas sensing, sensitivity

© 2022 Penerbit UTM Press. All rights reserved

## 1.0 INTRODUCTION

Exposure to gas may accidentally happen when there are industrial accidents, such as a leak from hazardous waste sites and underground tanks. According to Public Health Statement, the release of a gas substance will not eventually cause exposure to the human body unless one has come in contact with it through breathing, skin contact, or even by eating and drinking [1]. Other factors in determining whether one is harmed by exposure to gas are the amount of dosage, the period of contact, and the way of exposure. Being affected by a high level of carbon monoxide (CO) from vehicles, gas stoves, or tobacco smoke may kill a person since it harms the brain, lungs, and heart by limiting the amount of oxygen to reach the tissues [1]. Water contaminated with methane (CH<sub>4</sub>) gas will risk one's health or, in a serious case, may cause cancer [2]. Other harmful gases are benzene (C<sub>6</sub>H<sub>6</sub>) and carbon dioxide (CO<sub>2</sub>). Although benzene is widely used in the rubber manufacturing industry [3], being exposed to a high dosage will cause problems such as bone marrow deficiency, which eventually drops the number of red blood cells, causing anemia and many other harmful diseases [4]. Note that the effect of gas on human health depends on how much one is being exposed to. The same goes for carbon dioxide, where the blood and tissues' pH level decreases [5]. Therefore, having a device to detect the presence of hazardous gaseous is a need in today's community.

Fiber optics sensor technology has been utilized in various applications for almost a century with a variety of specifications and properties proposed by researchers to solve complex measuring problems and monitor parameters such as strain, temperature, pressure, and others [6-8]. The optical fiber sensor consists of a core and cladding with different refractive indices, where the light will be either transmitted to one end of the fiber or reflected back. Due to its features of light weight, immunity to electromagnetic interference, being very compact in size, and can easily embed into other structures, the optical fiber sensor is suitable to be utilized in composite materials since they are capable of condition monitoring of engineering structures [9,10]. One of the applications of optical fiber sensors is in gas sensing applications since the sensor is selective, non-destructive, and intrinsically safe in detection [11]. Several methods have been used in optimizing the gas sensor, such as redirection of light propagation in coupled resonant cavities [11], detection system based on non-dispersive infrared (NDIR) [12], and surface plasmon resonance (SPR) [13].

Surface plasmon resonance (SPR) was observed early in around 1900s, and the first SPR-based sensor was introduced in 1983 for biosensing and gas sensing [14]. It has been proven to be one of the best technologies since its first introduction in the early 1990s [15]. According to Sharma et al. (2007), the phenomena of SPR originated from Zenneck when he formulated a special surface wave solution to Maxwell's equations [16]. Sensors based on SPR have been widely developed since then in various fields and applications such as gas sensing [17], temperature sensing [18], urea detection [19], *Escherichia coli* (E-coli) identification [20], food quality [21] and monitoring water quality [22][23].

The development of the SPR sensor used a Kretschmann configuration consisting of a glass prism, metal thin film, and a light source. Glass prism couples light that passes through it and excites surface plasmon polariton (SPP) that can be generated through the conservation of energy and momentum [24]. Polariton is the interaction that occurs where photons interact with the polar excitation of electric dipoles in a semiconductor or at the metal's surface [25]. In addition, the refractive index and structure of the prism play a vital role in order to enhance the SPR signal. For example, the employment of a glass prism with  $n=1.51$  was found to generate an SPP excitation of about 8% compared to a prism with  $n=1.77$  [24]. In SPR excitation, the most used metals are either gold or silver due to their characteristics, where gold is highly stable in chemical and optical properties, while silver has a sharp SPR signal [13][26]. However, silver is easily oxidized compared to gold, thus making gold the most often metal used in SPR sensors [18]. Since the thickness of the metal thin film also influences the sensitivity of the SPR sensor, it is important to optimize the suitable thickness before being employed in the sensor. To generate maximum SPR signal amplification, the ideal thickness ranges from 40 nm to 60 nm [24]. An evanescent field might not appear if the metal film is too thick, or if it is too thin, it may result in electron-damping oscillations [27].

Due to the ability to generate strong SPR, a 50 nm thickness of the thin gold film was employed in this study. A thin film of a transition metal such as Cr and Ti is employed as a coating over the metal thin film (Au or Ag) to enhance its sensitivity and stability as well as withstand any harsh conditions. This work investigates the effect of light incident wavelength within the range of infrared and visible regions in detecting various types of gases which are benzene, methane, carbon monoxide, and carbon dioxide, using Winspall 3.02 simulation software. The gold thin film thickness was fixed at 50nm. Meanwhile, thicknesses of titanium varied between 1 nm to 5 nm throughout this study. It was found that different types of wavelength exhibit contrasted sensitivity performance for gas detection. The working principle of the proposed sensor is based on the detection of the refractive index of gases. In this work, the Winspall 3.02 software is used because it does not require a complicated simulation procedure yet is able to perform outstanding optical analysis using the Fresnel equation. The output of this study proves the bright potential of our proposed sensor for gas sensing applications due to its high sensitivity of up to 2412.06°/RIU and excellent selectivity in distinguishing different types of gases.

## 2.0 MATERIALS AND METHODS

This study was conducted using Winspall 3.02 simulation software based on the Fresnel equation [20]. Thin films were deposited on top of a glass prism (refractive index,  $n=1.5$ ), according to the Kretschmann configuration, as illustrated in Figure 1. The glass prism functions as a light coupler to ensure all light is successfully transmitted to the metal thin film so that a sufficient amount of energy is able to excite the surface plasmon polaritons (SPP). The first layer on top of the prism's hypotenuse side had been coated with a gold (Au) thin film ( $n=0.1758 + 3.4101k$ ) [27] with a thickness of 50 nm. Note that in this study, the Au thin film was fixed at the optimum thickness of 50nm, as explained in previous works [19, 28, 29]. The gold thin film was employed due to its stabilization and oxidization resistance compared to silver [30]. Titanium (Ti) thin film ( $n=2.6112 + 3.6024k$ ) with various thicknesses ranging from 1 nm to 5 nm was deposited on the Au thin film as the second layer to enhance the strength of plasmon excitation. A p-polarized incident light source was applied to the coated prism to generate the SPR signal.

Two different regions of light spectra, which are visible spectra ( $\lambda=400$  nm to  $\lambda=633$  nm) and infrared spectra ( $\lambda=870$  nm to  $\lambda=1550$  nm), were deployed. Four different types of gases such as benzene,  $C_6H_6$  ( $n=1.001762$ ); methane,  $CH_4$  ( $n=1.0004365$ ); CO ( $n=1.00025$ ) and  $CO_2$  ( $n=1.00043719$ ) were exposed on top of the coated glass prism. The characterization of the SPR signal was determined for each wavelength in both regions and various thicknesses of Ti for gas detection. SPR angle, minimum reflectance ( $R_{min}$ ), and angle shifting were crucial parameters that were investigated in order to obtain the best sensor sensitivity. The sensor's sensitivity was determined using Equation 1:

$$S = \frac{\Delta\theta}{\Delta RIU} \quad \text{---(Eq. (1))}$$

where  $\Delta\theta$  is the angle shifting and  $\Delta RIU$  and change of refractive index of the sensing medium. Theoretically, the sensing ability of the sensor was indicated by the presence of an evanescent field due to the excitation of surface plasmons [20]. The Au thin film successfully absorbed most of the incident light [27], thus leading to the presence of an evanescent field. The greater the amount of angle shifting, the better the sensitivity of the sensor [16].

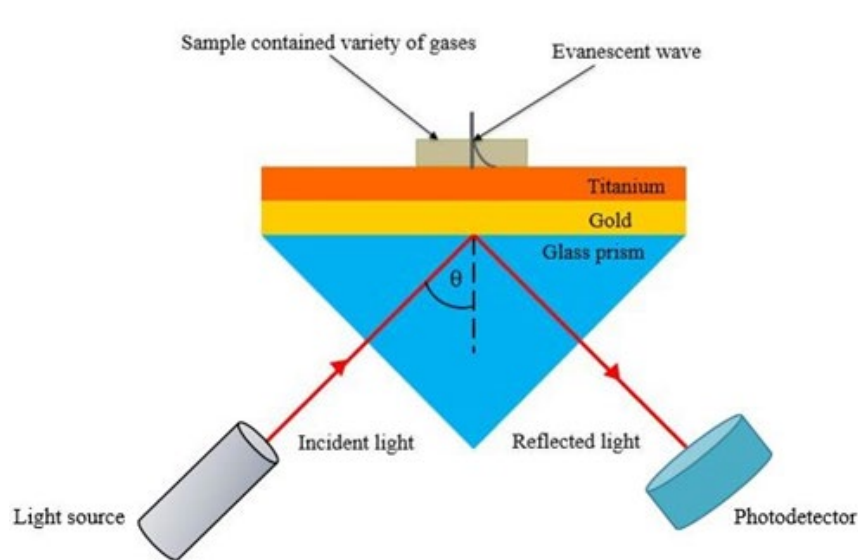


**Figure 1** Example of experimental setup consisting of the p-polarized light source (various excitation wavelengths), glass prism, metal thin films, and a sample of gases

**Table 1** Thicknesses and refractive indices for each material.

Material	Thicknesses (nm)	Refractive indices
Glass prism	-	1.51
Gold thin film	50	0.1758+3.4101k
Titanium coating	1-5	2.6112+3.6024k
Benzene gas	-	1.001762
Methane gas	-	1.0004365
Carbon monoxide	-	1.00025
Carbon dioxide	-	1.00043719
Air	-	1.0

**Table 2** Range of wavelength used in the p-polarized light source.

Regions	Wavelength (nm)						
Visible	400	440	480	520	560	600	633
Infrared	870	990	1110	1230	1350	1470	1550

### 3.0 RESULTS AND DISCUSSION

**Figure 2** illustrates the SPR curves as various wavelengths of visible light source were incident onto a 50 nm gold-coated prism with varying thickness of Ti from 1 nm to 5 nm, without the presence of gas samples. Note that SPR curve depth indicates the strength of the SPR signal. The deeper the dip, the stronger the SPP excitations [20]. As the thickness of Ti was set at  $t_{Ti}=1$  nm, the sharpest dip was obtained, as illustrated in **Figure 2(a)**, followed by  $t_{Ti}=2$  nm (**Figure 2(b)**). However, the SPR curve width became wider as the Ti thicknesses increased from  $t_{Ti}=3$  nm to  $t_{Ti}=5$  nm (**Figure 2(c-e)**). For example, at  $\lambda=400$  nm, a very

shallow SPR peak was obtained using Ti thin film with a thickness range from 3 nm (minimum reflectance,  $R_{\min}=0.77702$  a.u) to 5 nm ( $R_{\min}=0.79927$  a.u). Apparently, the deployment of very thin Ti film at 1 nm thickness ( $R_{\min}=0.703$  a.u) generated the most significant peak. When the wavelength increased to  $\lambda=440$  nm, the minimum reflectance was slightly reduced for all Ti thicknesses, with  $t_{\text{Ti}}=1$  nm possessing the smallest value. The same pattern was repeated where  $R_{\min}$  became smaller with the increment of excitation wavelength from  $\lambda=520$  nm to  $\lambda=633$  nm for each thickness. The lowest value of minimum reflectance was obtained as  $R_{\min}=0.13854$  a.u, achieved at  $\lambda=633$  nm with  $t_{\text{Ti}}=1$  nm. These results indicated that the maximum plasmon absorption in the visible region was successfully obtained when the wavelength was tuned to 633 nm.

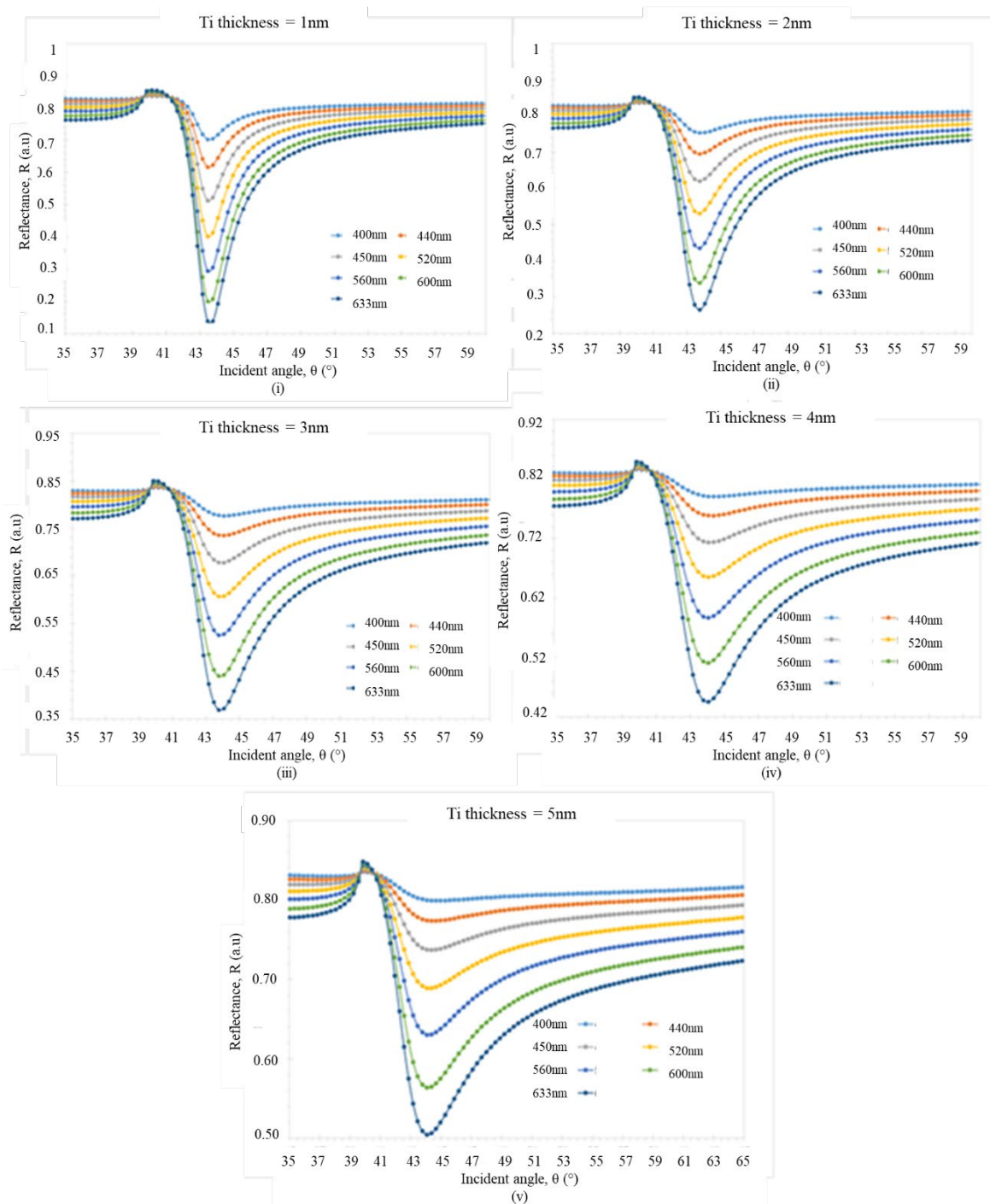


**Figure 2** SPR curves when the p-polarized light with various wavelengths in the visible spectrum was incident through the coated glass prism with various thicknesses,  $t$  of Ti (i)  $t_{\text{Ti}}=1$ nm, (ii)  $t_{\text{Ti}}=2$ nm, (iii)  $t_{\text{Ti}}=3$ nm, (iv)  $t_{\text{Ti}}=4$ nm and (v)  $t_{\text{Ti}}=5$ nm without the presence of the glass sample.

**Figure 3** displays the SPR curves as infrared (IR) light sources with various wavelengths were deployed. The values of  $R_{\min}$  decreased gradually as the wavelength increased in the visible region, in contrast with IR light. The sharpest dip of SPR curves was obtained at  $\lambda=870$  nm for  $t_{Ti}=1$  nm and  $t_{Ti}=2$  nm with  $R_{\min}$  values of 0.01714 a.u and 0.00274 a.u, respectively. For  $t_{Ti}=3$  nm, its minimum reflectance was observed at  $\lambda=990$  nm. Meanwhile, at  $t_{Ti}=4$  nm and  $t_{Ti}=5$  nm, both thicknesses achieved their lowest  $R_{\min}$  values at  $\lambda=1110$  nm. In comparison between the two types of light regions, the usage of IR wavelength produced better surface plasmon polaritons (SPP) excitations than visible light.

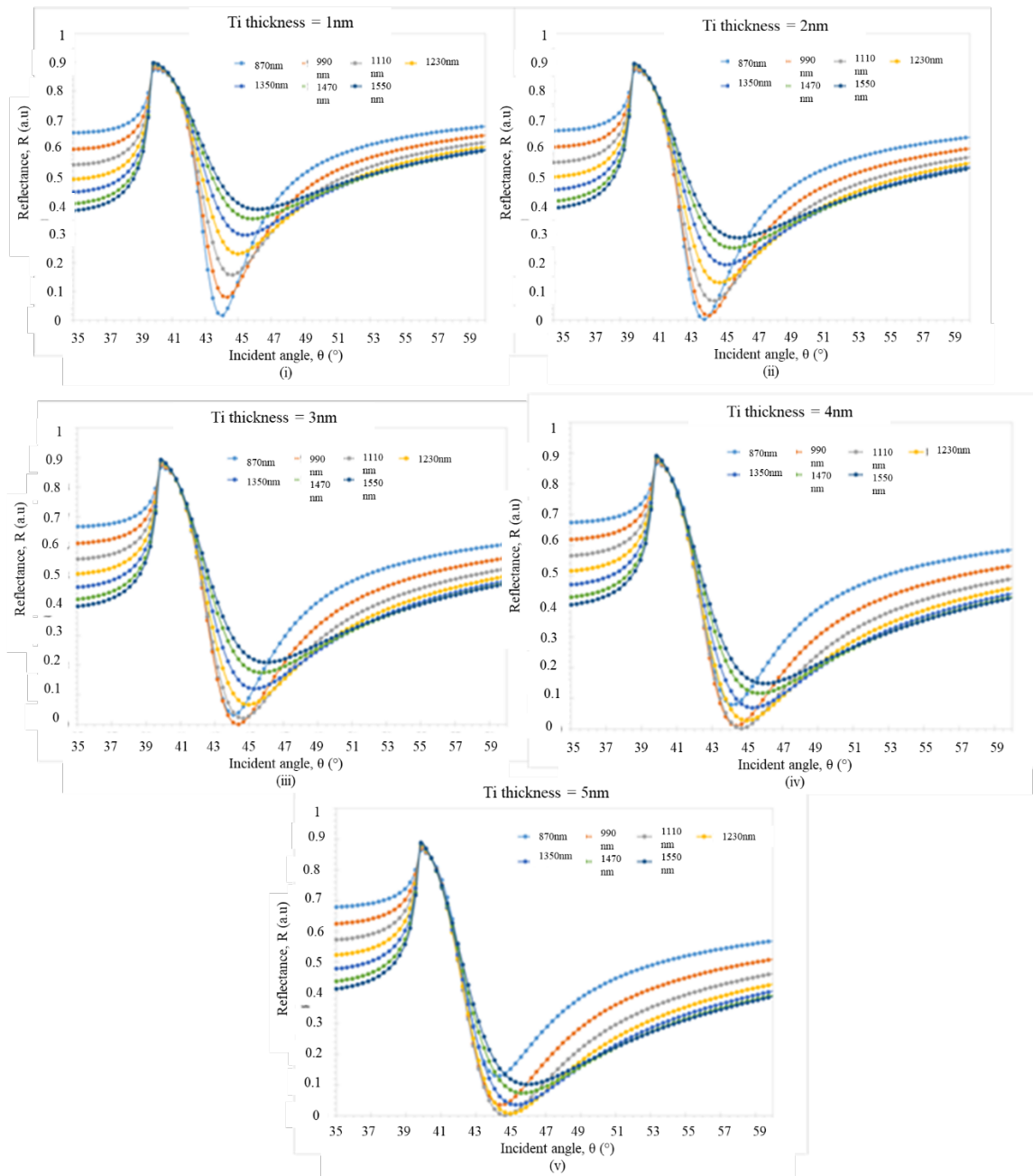


**Figure 3** SPR curves when the p-polarized light with various wavelengths in the infrared spectrum was incident through the coated glass prism with various thicknesses,  $t$  of Ti (i)  $t_{Ti}=1$  nm, (ii)  $t_{Ti}=2$  nm, (iii)  $t_{Ti}=3$  nm, (iv)  $t_{Ti}=4$  nm and (v)  $t_{Ti}=5$  nm without the presence of the gas sample.

**Figure 4** shows the variation of SPR curves with the presence of gases, for example, benzene ( $C_6H_6$ ). Overall, as the sensor detected the presence of gases using a visible light source, a slight decrement in minimum reflectance value was obtained as the wavelength increased from 400 nm to 633 nm. A different pattern was observed as the wavelength region was

shifted to the IR region. The lowest value of  $R_{\min}$  at  $\lambda=870$  nm was detected when Ti with thicknesses of 1 nm ( $R_{\min}=0.04096$  a.u) and 2 nm ( $R_{\min}=0.01705$  a.u) was used. As the wavelength was increased to 990 nm,  $t_{\text{Ti}}=3$  nm recorded the lowest value with  $R_{\min}=0.02649$  a.u. For  $t_{\text{Ti}}=4$  nm and  $t_{\text{Ti}}=5$  nm, their  $R_{\min}$  was obtained as 0.00699 a.u and 0.00489 a.u, respectively, at  $\lambda=1110$  nm. Similar patterns were observed for the other three types of gases ( $\text{CH}_4$ ,  $\text{CO}$ , and  $\text{CO}_2$ ). In terms of angle shifting, in general, both wavelength regions with thicknesses of Ti between 1 nm to 5 nm showed changes in SPR angle, indicating the capability of the proposed sensors to detect various types of gases. The usage of visible light source exhibited the same amount of angle shifting, which was  $0.30151^\circ$ . As the wavelength shifted to the IR region, most of the wavelength also showed the same values of angle shifting. However, few IR wavelengths resulted in high and significant angle shifting, such as at  $\lambda=990$  nm ( $\text{C}_6\text{H}_6$  detection),  $\lambda=1350$  nm ( $\text{CO}$  detection), and  $\lambda=1550$  nm ( $\text{CH}_4$ ,  $\text{CO}$ ,  $\text{CO}_2$  detections) due to their high optical absorption properties at these wavelengths.

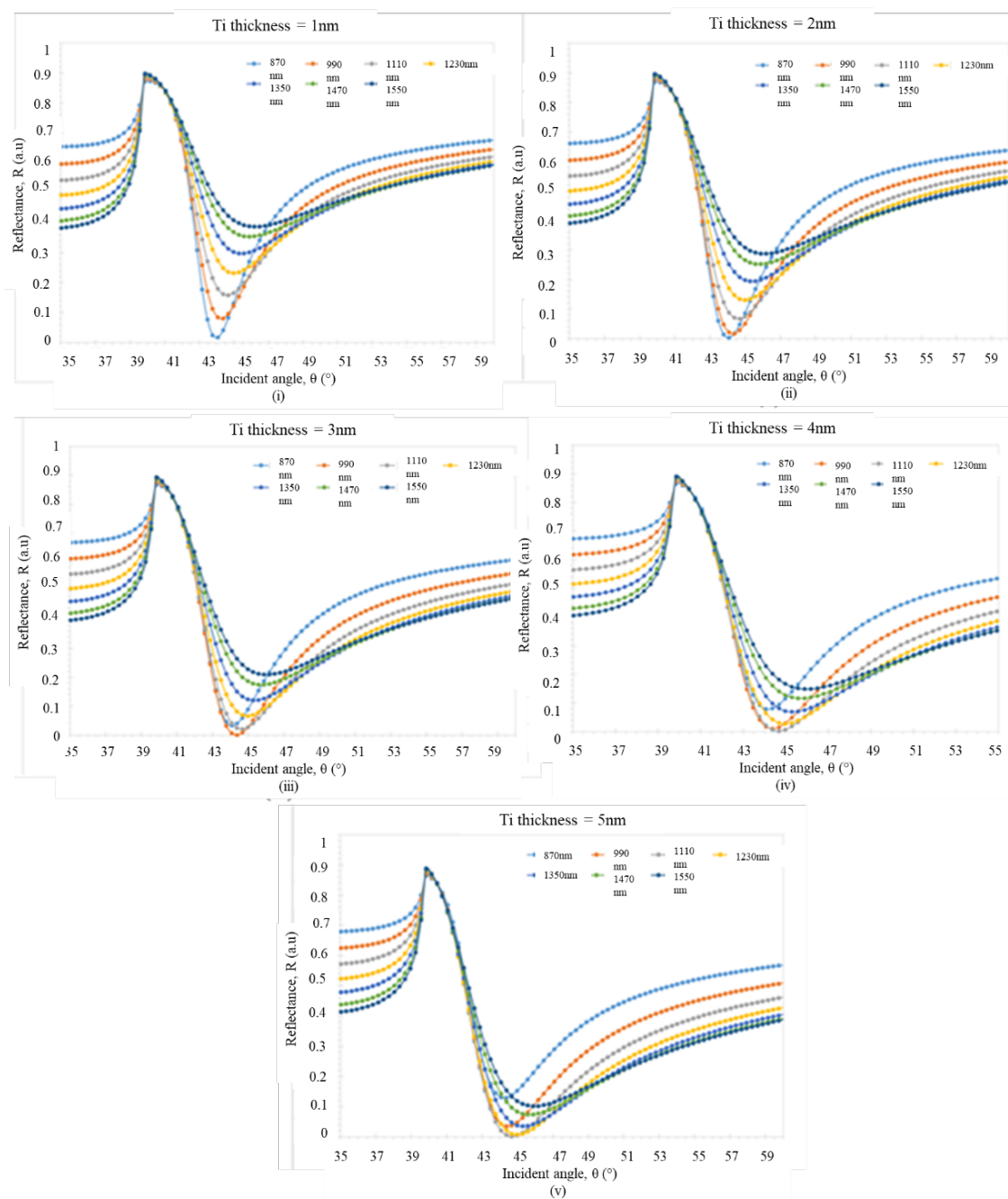


**Figure 4** SPR curves when the p-polarized light with various wavelengths in the infrared spectrum was incident through the coated glass prism with various thicknesses,  $t$  of Ti (i)  $t_{\text{Ti}}=1$  nm, (ii)  $t_{\text{Ti}}=2$  nm, (iii)  $t_{\text{Ti}}=3$  nm, (iv)  $t_{\text{Ti}}=4$  nm and (v)  $t_{\text{Ti}}=5$  nm with the presence of  $\text{C}_6\text{H}_6$  gas.

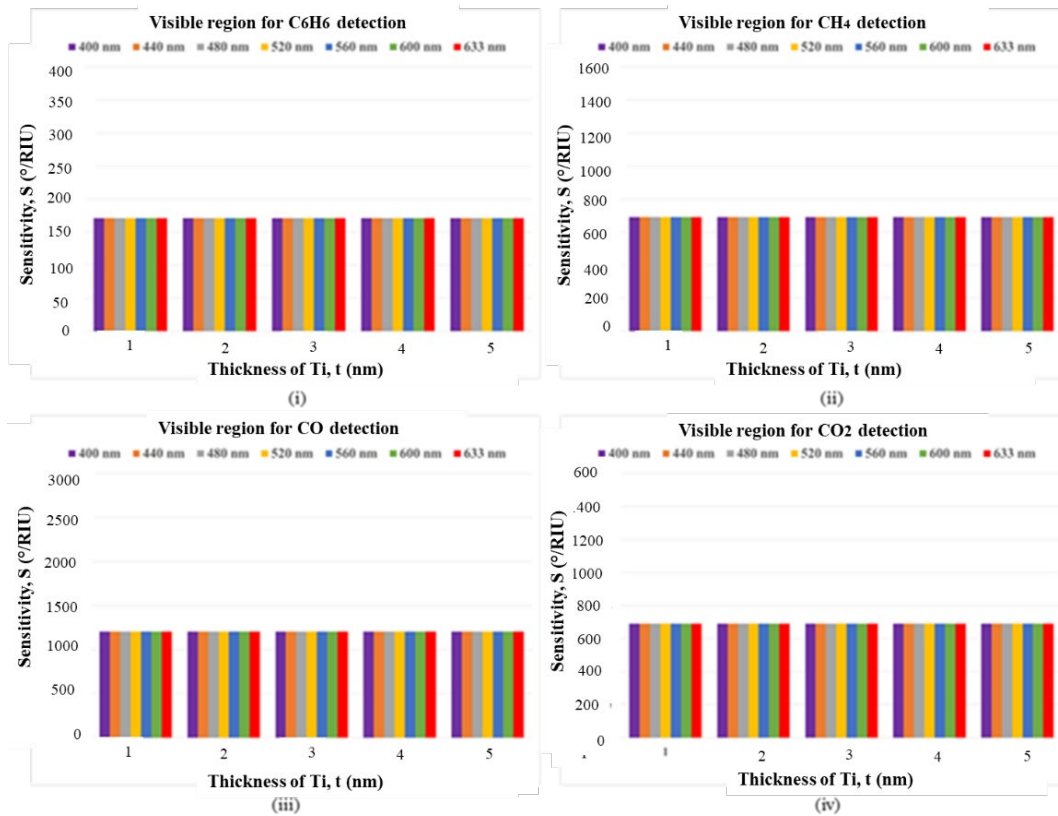


**Figure 5** Sensitivity of sensor for gaseous detection using wavelength in the visible region, (i)  $\text{C}_6\text{H}_6$ , (ii)  $\text{CH}_4$ , (iii)  $\text{CO}$ , (iv)  $\text{CO}_2$ .

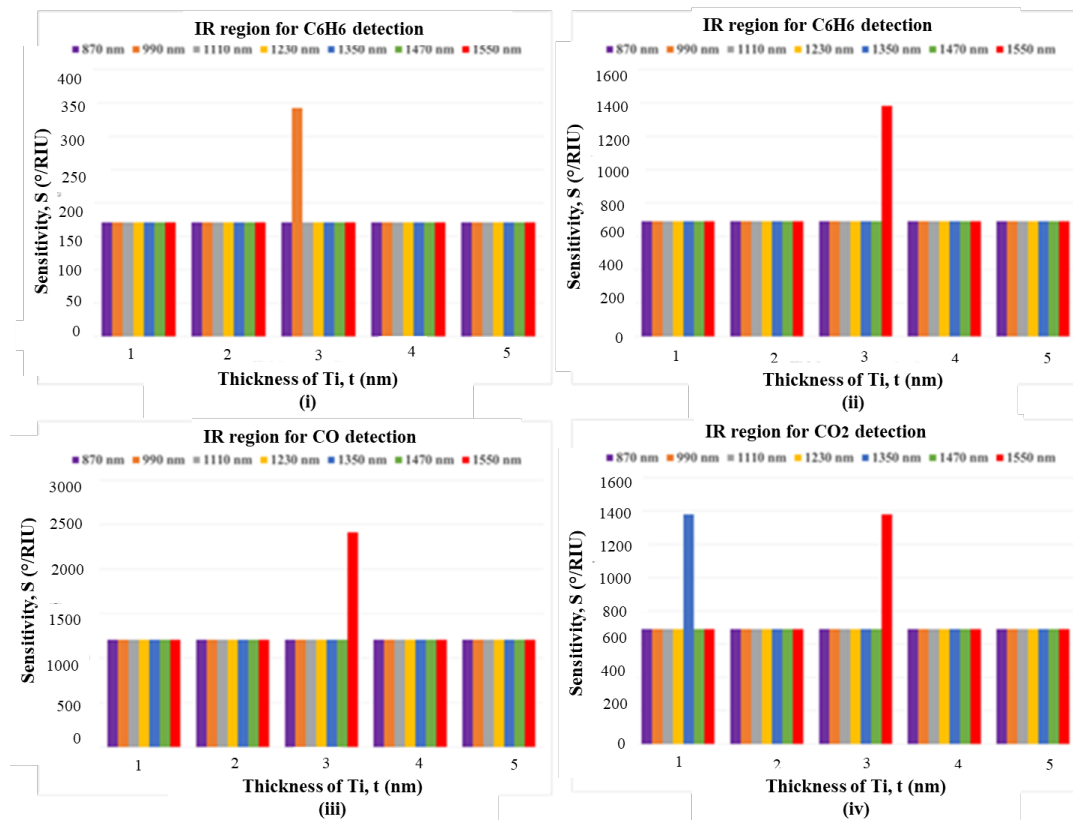


**Figure 6** Sensitivity of sensor for gaseous detection using wavelength in IR region, (i)  $\text{C}_6\text{H}_6$ , (ii)  $\text{CH}_4$ , (iii)  $\text{CO}$ , (iv)  $\text{CO}_2$ .

Figures 5 and 6 display the sensitivity analyses using visible and IR wavelengths, respectively, as the sensor is exposed to various types of gases. As displayed in Figure 5, the usage of operating wavelength ranging from  $\lambda=400$  nm to  $\lambda=633$  nm resulted in good sensitivity such as  $S=175.233^\circ/\text{RIU}$  ( $\text{C}_6\text{H}_6$  detection),  $S=753.231^\circ/\text{RIU}$  ( $\text{CH}_4$  detection),  $S=1203.145^\circ/\text{RIU}$  ( $\text{CO}$  detection) and  $S=751.255^\circ/\text{RIU}$  ( $\text{CO}_2$  detection). The ability to differentiate different types of gases indicate good selectivity performance of the proposed sensor. It is noteworthy to mention that the working principle of this sensor is based on the detection of the refractive index (RI) of the gases. Obviously, the RI values of  $\text{CO}_2$  and  $\text{CH}_4$  are almost similar, with a percentage difference of about 0.00012%, which explains why both sensitivities are nearly the same. It was found that the Ti thickness shows no significant role in enhancing the sensor's sensitivity, in which all thicknesses display the same sensitivity value. Nevertheless, there was a remarkable sensitivity value in the IR region, as depicted in Figure 6, where the deployment of  $t_{\text{Ti}}=3$  nm recorded the highest value for all gaseous detection. The value of sensitivity in benzene detection was  $340.233^\circ/\text{RIU}$  ( $\lambda=990$  nm), while methane and carbon monoxide possessed  $1381.48^\circ/\text{RIU}$  ( $\lambda=1550$  nm) and  $2412.06^\circ/\text{RIU}$  ( $\lambda=1550$  nm) respectively. For carbon dioxide sensing, it was observed that the two highest sensitivity values were  $1379.3^\circ/\text{RIU}$  at  $t_{\text{Ti}}=1$  nm ( $\lambda=1350$  nm) and  $t_{\text{Ti}}=3$  nm ( $\lambda=1550$  nm). Based on this analysis, it can be concluded that a high sensitivity and selectivity performance with excellent stability of the Au/Ti SPR sensor can be developed using  $\lambda=1550$  nm with  $t_{\text{Ti}}=3$  nm. Although other wavelength values (IR and visible region) indicate a good sensitivity, an outstanding sensitivity had been obtained at the optical communication wavelength,  $\lambda=1550$  nm, due to its high optical absorption properties.

The sensitivity comparison between the highest sensitivity sensor ( $\lambda=1550$  nm,  $t_{\text{Ti}}=3$  nm) and other sensitivities (all wavelengths except 1550 nm at thicknesses of Ti between 1 nm to 5 nm) is depicted in Figure 7. Obviously, to achieve maximum sensitivity, the selection of suitable wavelength and thickness of Ti plays an important role. The total thin film thickness of 53 nm (gold (50 nm) + Ti (3 nm)) is the optimum thickness to generate a strong SPR signal. Note that too thin of thin film produces electron damping situation. Meanwhile, if the film is too thick, the SPR signal is unable to be generated due to the photon absorption by the material itself [30]. Table 3 presents the sensitivity performance comparison between our work and previous studies. It appears that the deployment of the 1550 nm wavelength resulted in better sensitivity compared with 633 nm. Material selection is an important parameter in developing high-sensitivity SPR sensors. Evidently, our proposed Au/Ti sensor exhibits the highest sensitivity up to  $2412^\circ/\text{RIU}$  with a less complicated configuration structure.

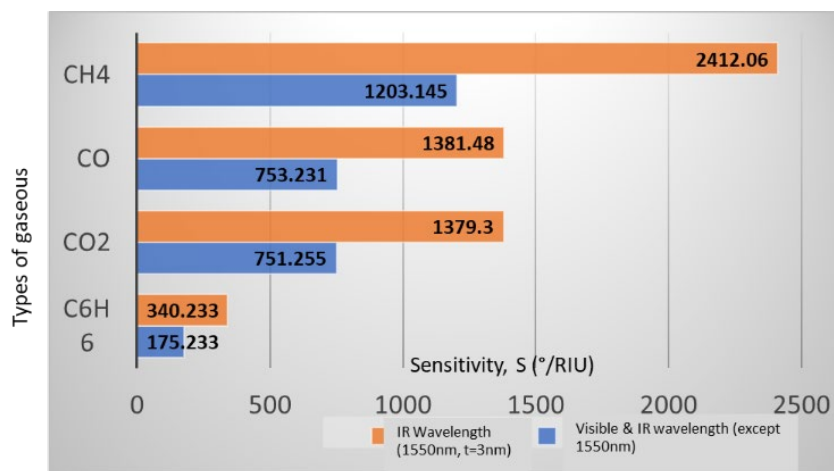


Figure 7 Sensitivity of sensor for gaseous detection using wavelength in IR region, (i)  $\text{C}_6\text{H}_6$ , (ii)  $\text{CH}_4$ , (iii)  $\text{CO}$ , (iv)  $\text{CO}_2$ .

Table 3 Sensitivity comparison between our proposed sensor and previous works.

Wavelength	Sensitivity ( $^\circ/\text{RIU}$ )	Thickness	Configuration
633nm	6	53 nm	Cu/Chitosan [31]
1550nm	119	50 nm	CaF2 prism/Al/BTO/Al/MoS2 [32]
1550nm	2412	53 nm	Au/Ti

#### 4.0 CONCLUSION

The Au/Ti are promising hybrid materials for SPR-based gas sensing applications. The proposed Au/Ti based-SPR sensor with thicknesses of Ti within 1 nm to 5 nm using visible and IR wavelengths able to detect various types of gaseous. Highly selectivity



and sensitivity SPR sensor up to 2412.06°/RIU was successfully developed using infrared (IR) wavelength at  $\lambda=1550$  nm at Ti thickness of 3 nm. Obviously, this sensor is able to distinguish small refractive index differences between the gases, which indicates its outstanding selectivity criterion.

## Acknowledgment

The Faculty of Science and Technology (FST) and Universiti Sains Islam Malaysia (USIM) are acknowledged for their research facilities.

## References

- [1] Agency for Toxic Substances and Disease Registry (ATSDR), "Public Health Statement Carbon Monoxide - Division of Toxicology and Human Health Sciences," no. June, 2016, [Online]. Available: [www.atsdr.cdc.gov/](http://www.atsdr.cdc.gov/)
- [2] H. Mohajan, "Dangerous Effects of Methane gas in the Atmosphere," *J. Econ. Polit. Integr.*, vol. 2, no. 1, pp. 3–10, 2012.
- [3] D. Galbraith, S. A. Gross, and D. Paustenbach, "Benzene and human health: A historical review and appraisal of associations with various diseases," *Crit. Rev. Toxicol.*, vol. 40, no. SUPPL. 2, pp. 1–46, 2010, doi: 10.3109/10408444.2010.508162.
- [4] Z. A. Kasemy, G. M. Kamel, G. M. Abdel-Rasoul, and A. A. Ismail, "Environmental and health effects of benzene exposure among Egyptian taxi drivers," *J. Environ. Public Health*, vol. 2019, 2019, doi: 10.1155/2019/7078024.
- [5] P. Bierwirth, "Carbon Dioxide Toxicity and Climate Change: A Serious Unapprehended Risk for Human Health," *Res. Gate Work. Pap.*, no. May, pp. 1–22, 2020, doi: 10.13140/RG.2.2.16787.48168.
- [6] D. Krohn, "Fiber Optic Sensors : Fundamentals and Applications," 2015.
- [7] B. Culshaw, "Optical Fibre Sensors : A Current Perspective," pp. 21–31, 2013.
- [8] J. Castrellon-uribe, "Optical Fiber Sensors : An Overview Optical Fiber Sensors : An Overview," no. January, 2015, doi: 10.5772/28529.
- [9] X. W. Ye, Y. H. Su, and J. P. Han, "Structural Health Monitoring of Civil Infrastructure Using Optical Fiber Sensing Technology : A Comprehensive Review," vol. 2014, 2014, <https://doi.org/10.1155/2014/652329>.
- [10] C. Materials, "Overview of Fiber Optic Sensor Technologies for Strain / Temperature Sensing Applications in," 2016, doi: 10.3390/s16010099.
- [11] C. E. Campanella, M. De Carlo, A. Cuccovillo, F. De Leonardis, and V. M. N. Passaro, "Methane Gas Photonic Sensor Based on Resonant Coupled Cavities," *Sensors*, vol. 19, no. 23, pp. 5171, 2019, <https://doi.org/10.3390/s19235171>.
- [12] Q. Tan, L. Tang, M. Yang, C. Xue, and W. Zhang, "Three-gas detection system with IR optical sensor based on NDIR technology," *Opt. Lasers Eng.*, vol. 74, pp. 103–108, 2015, doi: 10.1016/j.optlaseng.2015.05.007.
- [13] A. L. C. M. D. Silva, M. G. Gutierrez, A. Thesing, R. M. Lattuada, and J. Ferreira, "SPR biosensors based on gold and silver nanoparticle multilayer films," *J. Braz. Chem. Soc.*, vol. 25, no. 5, pp. 928–934, 2014, doi: 10.5935/0103-5053.20140064.
- [14] B. A. Prabowo, "Surface Plasmon Resonance Optical Sensor: A Review on Light Source Technology," doi: 10.3390/bios8030080.
- [15] H. H. Nguyen, J. Park, S. Kang, and M. Kim, "Surface Plasmon Resonance: A Versatile Technique for Biosensor Applications," pp. 10481–10510, 2015, doi: 10.3390/s150510481.
- [16] A. K. Sharma, R. Jha, and B. D. Gupta, "Fiber-optic sensors based on surface plasmon resonance: A comprehensive review," *IEEE Sens. J.*, vol. 7, no. 8, pp. 1118–1129, 2007, doi: 10.1109/JSEN.2007.897946.
- [17] A. Paliwal, A. Sharma, M. Tomar, and V. Gupta, "Carbon monoxide ( CO ) optical gas sensor based on ZnO thin films," *Sensors Actuators B. Chem.*, 2017, doi: 10.1016/j.snb.2017.05.064.
- [18] R. Zhang, S. Pu, and X. Li, "Gold-film-thickness dependent SPR refractive index and temperature sensing with hetero-core optical fiber structure," *Sensors (Switzerland)*, vol. 19, no. 19, 2019, doi: 10.3390/s19194345.
- [19] P. Susthitha Menon *et al.*, "High Sensitivity Au-based Kretschmann Surface Plasmon Resonance Sensor for Urea Detection (Sensor Resonans Plasmon Permukaan Kretschmann berasaskan Au Berkepekaan Tinggi untuk Pengesanan Urea)," *Sains Malaysiana*, vol. 48, no. 6, pp. 1179–1185, 2019, [Online]. Available: <http://dx.doi.org/10.17576/jsm-2019-4806-04>
- [20] W. M. Mukhtar, "E-coli identification using Kretschmann-based Ag/GO nanocomposites plasmonic sensor," *AIP Conf. Proc.*, vol. 2203, no. January, pp. 1–8, 2020, doi: 10.1063/1.5142094.
- [21] K. Narsaiah, S. N. Jha, and R. Bhardwaj, "Optical biosensors for food quality and safety assurance — a review," vol. 49, no. August, pp. 383–406, 2012, doi: 10.1007/s13197-011-0437-6.
- [22] X. Jiang and Q. Meng, "Design of Optical Fiber SPR Sensing System for Water Quality Monitoring," vol. 1, no. Iccse, pp. 123–127, 2015, doi: 10.2991/iccse-15.2015.21.

- [23] W. M. Mukhtar, R. Mohd Halim, K. Ahmad Dasuki, A. R. Abdul Rashid, and N. A. Mohd Taib, "SPR sensor for detection of heavy metal ions: Manipulating the EM waves polarization modes," *Malaysian J. Fundam. Appl. Sci.*, vol. 13, no. 4, pp. 619–622, 2017, doi: 10.11113/mjfas.v13n4.748.
- [24] W. M. Mukhtar, R. M. Halim, and H. Hassan, "Optimization of SPR signals: Monitoring the physical structures and refractive indices of prisms," vol. 01001, 2017, doi: 10.1051/epjconf/201716201001.
- [25] M. S. A. Gandhi, S. Chu, K. Senthilnathan, P. R. Babu, and K. Nakkeeran, "applied sciences Recent Advances in Plasmonic Sensor-Based Fiber Optic Probes for Biological Applications," 2019, doi: 10.3390/app9050949.
- [26] G. Wang, C. Wang, R. Yang, W. Liu, and S. Sun, "A sensitive and stable surface plasmon resonance sensor based on monolayer protected silver film," *Sensors (Switzerland)*, vol. 17, no. 12, 2017, doi: 10.3390/s17122777.
- [27] W. M. Mukhtar, N. F. Murat, N. D. Samsuri, and K. A. Dasuki, "Maximizing the response of SPR signal: A vital role of light excitation wavelength," *AIP Conf. Proc.*, vol. 2016, no. September, 2018, doi: 10.1063/1.5055506.
- [28] S. Fouad, N. Sabri, Z. A. Z. Jamal, and P. Poopalan, "Surface plasmon resonance sensor sensitivity enhancement using gold-dielectric material," *Int. J. Nanoelectron. Mater.*, vol. 10, no. 2, pp. 147–156, 2017.
- [29] S. K. Srivastava, "Fiber Optic Plasmonic Sensors: Past, Present and Future," *Open Opt. J.*, vol. 7, no. 1, pp. 58–83, 2014, doi: 10.2174/1874328501307010058.
- [30] W. M. Mukhtar, S. Shaari, A. A. Ehsan, and P. S. Menon, "Electro-optics interaction imaging in active plasmonic devices," *Opt. Mater. Express*, vol. 4, no. 3, p. 424, 2014, doi: 10.1364/ome.4.000424.
- [31] W. M. Mukhtar, N. A. M. Taib and A. R. A. Rashid, "Sensitivity Analyses of Cu/Chitosan and Ag/Chitosan Based SPR Biosensor for Glucose Detection," *Journal of Physics: Conference Series*, vol. 1892, no. 1, 2021, doi: <https://doi.org/10.1088/1742-6596/1892/1/012021>.
- [32] S. Shukla, N. Grover and P. Arora, "Resolution enhancement using a multi-layered Aluminum-based plasmonic device for chikungunya virus detection," 2022, (Under review), doi: <https://doi.org/10.21203/rs.3.rs-1752532/v1>.